Optimal Pilot Placement in Cognitive Radio Systems for Wiener Filtered MMSE Channel Estimation

Boyan V. Soubachov
Department of Electrical Engineering
University of Cape Town
Rondebosch, Cape Town, South Africa
e-mail: boyan@crg.ee.uct.ac.za

Neco Ventura
Department of Electrical Engineering
University of Cape Town
Rondebosch, Cape Town, South Africa
e-mail: neco@crg.ee.uct.ac.za

***Abstract*—Non-contiguous Orthogonal Frequency Division Multiplexing (NC-OFDM) Cognitive Radios (CRs) pose an intriguing situation for optimal pilot-pattern generation. It has been proposed that in order to attain the lowest possible Mean Squared Error (MSE) of a channel estimator, the pilots should be placed adjacent to an interfering Primary User (PU) to allow for the highest pilot to data symbol cross-correlation and the lowest pilot auto-correlation. In past research, this has been shown to provide a significant decrease in the channel estimator's MSE; moreover the optimal power loading required such that the PU does not experience interference above a certain threshold from the Secondary User (SU) is not taken into account. This leads to a contradiction between the optimal power loading and the optimal pilot pattern. In this paper, the relationship between these two concepts is investigated with the implementation of a Minimum Mean Squared Error (MMSE) Wiener filter and the optimal pilot positioning is derived.**

Keywords-OFDM; cognitive radio; MMSE estimation; power loading

I. INTRODUCTION

Bearing in mind the practical limits of higher frequency ranges, spectrum scarcity has become a great issue. This is further exacerbated by the immense growth of services and protocols which demand an ever increasing link speed. It has thus become of great importance to achieve as high a spectral efficiency as possible when engineers design the next generation wireless communications systems and standards.

A solution widely accepted as a spectrally efficient and practical alternative to spectrum re-arrangement is cognitive radio. Cognitive radio works on the basis of an intelligent software-defined radio (SDR) where a CR user (also known as the secondary user) transmits in licensed (or primary user) frequency bands when the licensed user themselves are not transmitting [1]. This solution promises to be an almost ideal alternative since, in a perfect implementation, the entire usable spectrum would be fully utilised.

The call for cognitive radios is further backed by research and surveys done on spectral usage in typical geographic areas. It has been noted that even though much of the usable spectrum has been occupied and licensed, it is only used anywhere from 15% to 85% of the time in a wide geographic and time dispersion [2]. This can be even lower in certain situations such as sub-urban environments where frequency utilisation from 100 MHz to 3 GHz can be utilised as little as 7% of the time [3]. An interpretation which can derived from this is that much of the usable spectrum is reserved for licensed operation but is only used by its licensees a very small percentage of the time or that its actual licensed use is limited to a relatively small geographical area.

It is commonly proposed that a non-contiguous OFDM system be used to implement a CR system. This allows the sub-channels of an OFDM system which interfere with the primary user to be switched off. This means that the NC-OFDM system would comply with one of the principles of CR such that any CR-compliant communications are transparent to, and need not be considered by, non CR-compliant systems.

In this paper, the related work in the fields of optimal power loading and optimal pilot patterns is described in Section II. The system model used to derive the proposed solution is described in Section III and the proposed solution itself is derived in Section IV. The simulation results are shown and discussed in Section V and a conclusion is drawn in Section VI.

II. RELATED WORK

In related work, two aspects of CR research focus on the optimal pilot patterns and the optimal power loading for secondary users. In [4] the optimal power loading is investigated for CR users such that power loaded to the individual sub-channels (which are then assigned to SUs) is such that interference to PUs, which are adjacent to the SUs, is kept below a threshold value as specified by design. It found in [4] that the optimal power loading profile which maintains interference to the PU below a threshold is that of a 'step' profile, meaning that less power is allocated to sub-channels closer to the PU and more power is allocated to sub-channels farther away from a PU.

The optimal pilot pattern for the SU in a cognitive radio environment is investigated in [5]. It was found that when a PU initially starts transmitting it is optimal to convert the sub-channels adjacent to the PU's transmission band to pilot sub-channels. This is such that the cross-correlation between pilot and data symbols is maximised (as the addition of an

 ISBN: 978-1-61208-131-1

extra pilot sub-channel can only increase the cross-correlation) and the auto-correlation between pilot sub-channels is decreased. It is also noted that the MSE of the estimator also depends on the signal-to-noise ratio (SNR) of the received pilot symbols [5].

These two aspects are both optimal in their own sense but it was found that they crucially fail to consider their common dependence. While the optimal pilot pattern proposes that an extra pilot be placed adjacent to the PU (with MSE decreasing as the pilot sub-channel is moved closer to the PU) it is not considered that the SNR of the pilot symbols in the sub-channel may only decrease due to the decrease in transmission power for the pilot bearing sub-channel as necessitated by the optimal power loading algorithm. This contradiction is further exacerbated by the fact that a PU would, in most practical situations, be non-orthogonal to the SU and therefore the SU would have a higher noise floor on sub-channels closer to the PU, additionally reducing the SNR available for pilot sub-channels.

A further addition to the problem is the principle of boosting the power for pilot symbols. This is characterised as the pilot-to-data power ratio (PDPR) and the point behind it being that a lower estimator MSE can be achieved by allocating more power to pilot symbols than which is normally allocated to data symbols.

Research done on this contradiction, as presented in this paper, has led to the development of a solution where the optimal pilot pattern is achieved while maintaining the optimal power loading profile such that interference to the PU is kept below a desired threshold. The channel estimation method used is the MMSE criterion implemented as the Wiener finite impulse response (FIR) filter.

III. SYSTEM MODEL

The model used to simulate the CR system is that of an OFDM transmission of N sub-channels having N_d carriers disabled due to an interruption caused by a PU. This allows spectrum to be fully utilised since there would be no guard-bands between the PU's and the SU's signal.

The system is considered to have allocated a total of N_p sub-channels for the sole purpose of transmitting pilots. For the sake of simplicity, the system is analysed using a 1-dimensional pilot pattern in frequency only. As prescribed in [6], the system differentiates between PU-to-SU and SU-to-PU interference for the purposes of optimal power loading.

A. Power density spectrum of signals

The transmitted signals in the system model are assumed, for the sake of simplicity, to be shaped by a rectangular pulse shaping function. The power density spectrum of the rectangular pulse shaping function can be represented as [4]

$$\phi_i(f) = P_i T_s \left(\frac{\sin(f \cdot \pi \cdot T_s)}{f \cdot \pi \cdot T_s} \right)^2 . \qquad (1)$$

In (1), P_i represents the transmit power of the i_{th} sub-carrier and T_s represents the symbol duration of that same sub-carrier. It would serve well to note that the equation is only applicable to a rectangular pulse-shaping function and is used for simplicity. Other equations may be substituted for (1) but the contradiction (and therefore solution) will still hold since all non-ideal filters have some form of spectral roll-off and therefore present interference to adjacent frequency bands.

B. Interference from PU to SU

The signals between PU and SU are assumed to be non-orthogonal and therefore the interference imposed on a SU by a PU is effectively 'smeared' due to the Fast Fourier Transform (FFT) performed by the SU [6]. The expected value of the power density spectrum of the PU's signal after an FFT of size M is performed can be described as [6]

$$E\{I_M(\omega)\} = \frac{1}{2\pi M} \int_{-\pi}^{\pi} \phi_{PU}(e^{j\omega}) \left(\frac{\sin(\omega - \psi)M/2}{\sin(\omega - \psi)/2} \right)^2 d\psi \qquad (2)$$

where ω represents the angular frequency which has been normalised to the sampling frequency and $\phi_{PU}(e^{j\omega})$ represents the power density spectrum of the PU's pulse-shaping filter.

The interference from the PU to the SU can then be described as the integral of the expected value of the power spectral density, which may be expressed as

$$I_{PU}(d_i, P_i) = \int_{d_i - \Delta f/2}^{d_i + \Delta f/2} E\{I_M(\omega)\} d\omega \qquad (3)$$

In (3), d_i represents the spectral distance between the considered sub-carrier and the PU and Δf represents the width of one sub-channel of the SU (equivalent to the inverse of the OFDM symbol duration).

C. Interference from SU to PU

The interference from the secondary user to the primary user is modelled using simpler mathematics due to the assumption that we do not have any information about the PU's modulation scheme and other transmission properties, only the bandwidth and signal power.

The interference caused by spectral roll-off from the SU can then be simply modelled as the integration of the power density spectrum of the signal, represented as (1) for the rectangular pulse shaping filter case. The interference from the SU can therefore be modelled as [4]

 ISBN: 978-1-61208-131-1

$$I_{SU}(d_i, P_i) = \int_{d_i - B/2}^{d_i + B/2} \phi_i(f) df. \quad (4)$$

It should be noted that B denotes the bandwidth occupied by the PU's signal such that the integration is performed over the PU's bandwidth with an added frequency 'offset' introduced by the spectral distance between the considered sub-channel and the PU's signal.

D. Optimal power loading

The optimal power loading algorithm is specified in [4]. It is important to note that the same power loading algorithm is derived at the boundary level where the interference to the PU is equal to the interference threshold parameter such that transmission power is maximized and, consequently, so is channel capacity.

It is noted in [4] that this is indeed the optimal point for the power loading algorithm since the channel capacity of a sub-channel is proportional to the power loaded to said sub-channel. The interference equation at the threshold was therefore used such that the equation is formulated as

$$P_i^* = \frac{I_{th}}{\frac{\partial I_{SU}}{\partial P_i}}. \quad (5)$$

where I_{th} is the power threshold of the interference introduced into the primary user's band by the secondary user.

E. Estimator correlation and Wiener filter MMSE

One of the ways in which a channel frequency response (CFR) can be estimated and interpolated is through the use of a Wiener FIR filter [7]. The optimal Wiener filter allows us to achieve the MMSE criterion for the channel estimator by utilizing statistics about the channel, specifically the channel's auto- and cross-correlation data.

The frequency cross-correlation between pilot and data symbols where a rectangular Doppler spectrum is assumed is given as [7], [8]

$$\theta_{\Delta f}(d_{dp}) = \frac{\sin(2\pi\tau_{\max}\Delta f d_{dp})}{2\pi\tau_{\max}\Delta f d_{dp}}. \quad (6)$$

In equation (6), $\tau_{\max}$ represents the maximum expected delay of the channel, Δf represents the sub-channel width or carrier spacing and d_{dp} represents the integer distance between the pilot and the data sub-channel to which the cross-correlation needs to be calculated.

The auto-correlation function between different pilot symbols is also needed to compute the optimal Wiener FIR filter coefficients. The auto-correlation function for the pilot symbols is given as [7], [8]

$$\phi(d_{pp'}) = \theta_{\Delta f}(d_{pp'}) + \frac{\sigma_n^2}{E\{|S(n_{p'})|^2\}}, \quad (7)$$

where $d_{pp'}$ represents the integer distance (sub-channel multiples) between two neighbouring pilot symbols in the frequency dimension, σ_n^2 represents the mean noise variance between pilot symbols and $E\{|S(n_{p'})|^2\}$ represents the mean energy of the pilot symbols.

For the implementation of the MMSE filter, the derivative of the MSE function needs to be set to zero such that we achieve the filter coefficients which achieve the minimum possible MSE. The MMSE for the Wiener filter is derived as [7]

$$J_{n,i} = E\{|H_{n,i}|^2\} - \boldsymbol{\theta}_{n,i}^T \boldsymbol{\phi}^{-1} \boldsymbol{\theta}_{n,i}^* \quad (8)$$

where $\boldsymbol{\theta}$ and $\boldsymbol{\phi}$ represent the cross- and auto-correlation matrices respectively. However, since we are dealing with the single dimensional estimator (frequency only) the cross- and auto-correlation matrices reduce to vectors [7] and therefore can be simplified to element-wise multiplication and inversion.

IV. Optimal Solution

In order to obtain the optimal pilot placement, the pilot needs to be placed in the sub-channel which allows for the lowest MMSE out of the possible sub-channels for pilot placement. Given that the MMSE is defined as always positive [7] it would mean that the pilot placement needs to be found where

$$\boldsymbol{\varepsilon} = -\boldsymbol{\theta}_n \boldsymbol{\phi}^{-1} \boldsymbol{\theta}_n \quad (9)$$

is a maximum. It should be noted that, in (9), since the estimator is 1-dimensional for these purposes and the filter coefficients are strictly real [7], the error vector $\boldsymbol{\varepsilon}$ is obtained without any conjugation and using only element-wise multiplication and inversion.

The optimisation problem can therefore be written as

$$\min \varepsilon = -\frac{\left[\theta_{\Delta f}(d_{dp})\right]^2}{\theta_{\Delta f}(d_{pp'}) + \frac{2(\sigma_n^2 + I_{PU})}{P_i^*}}. \quad (10)$$

The error function as specified by (9) and (10) is used to determine where the optimal placement of the new pilot would be. The functions are chosen such as to represent the change in MSE relative to the SU's system without adding a new pilot. The MSE change in (10) is evaluated only over 2 pilot sub-channels, therefore MSE difference is only compared to the nearest pilot instead of all pilots. This is due to the linear scaling of the MSE difference between a localised, 2-pilot model and an evaluation over all pilots and so the optimal calculation is done over the nearest, unmoved pilot and the proposed positioning of the new pilot. Since the SNR expression in (7) represents the average SNR over all

 ISBN: 978-1-61208-131-1

pilots, the term is then adjusted in (10) so that the SNR contribution added by the new pilot is divided by a factor of two. This allows the error function value to be either positive or negative in that a negative error function value would represent a decrease in the overall estimation MMSE whereas a positive value would represent an overall increase in the estimation MMSE.

The proof to this logical decision is simple in that the MMSE of the Wiener filter as demonstrated in (8) depends on the auto-correlation of pilot symbols (ϕ). For a two-dimensional system, the matrix depends on the nearest pilot symbols in both time and frequency but in the one-dimensional case (be it either time or frequency) the matrix becomes a vector and the values are then only dependent on the two nearest pilot symbols on either side of the pilot symbol concerned.

It would serve well to note that the function described in (10) is transcendental in nature and therefore has no algebraic form solution for its derivative. Techniques such as the Karush-Kuhn-Tucker (KKT) conditions cannot be used to find an equation for the optimal position. The solution, therefore, has to be found using enumeration over the problem space or through a numerical solution.

At first thought, it would seem computationally expensive to search for the optimal pilot positioning (where the MMSE error function is lowest) by brute-force enumeration. This is however not the case since the error function is bound to a problem space which is single dimensional (vector space) and, at most, has a length equal to the pilot interval of the original pilot pattern. Another advantage is that the pilot auto-correlation values can be pre-computed and stored after the first iteration for obtaining the optimal error function since the pilot symbols are of a known sequence.

V. SIMULATION PARAMETERS AND RESULTS

In order to simulated the system an NC-OFDM cognitive radio receiver was simulated using the parameters as described in Table 1. It should be noted that the narrowband and wideband PU interference parameters are specified as a percentage of the PU's power.

The system was simulated by averaging the results over 10000 runs such that a statistically significant sample was achieved and an appropriate conclusion could be inferred. The system simulated first was that of a wideband system where the PU's spectrum was set to be 20 times the bandwidth of a single SU sub-channel.

It was noted that due to the mathematical formulation of the SU-to-PU interference, the width of the PU plays a large role in determining the optimal pilot positioning. This is due to the summation caused by the integral, effectively meaning that PUs with a larger bandwidth are more sensitive to interference effects and spectral roll-off introduced by the SU. This meant that in implementing the error function and obtaining the optimal pilot placement, lower interference thresholds could be used for the narrowband case (where the PU's band is assumed to be of the same bandwidth as 1 pilot sub-channel).

TABLE I. SIMULATION PARAMETERS

Parameter	Value
PU transmit power	1 mW
Maximum delay spread (τ_{max})	10 µs
FFT size	512
PU bandwidth	625 (20 Δf) kHz
SU transmit power	1 mW
SU sub-channel bandwidth (Δf)	31.25 kHz
Noise floor	-90 dBm
Pilot spacing (sub-channels)	9
Wideband interference thresholds	[25; 10; 5; 1] %
Narrowband interference thresholds	[0.25; 0.1; 0.05; 0.01] %

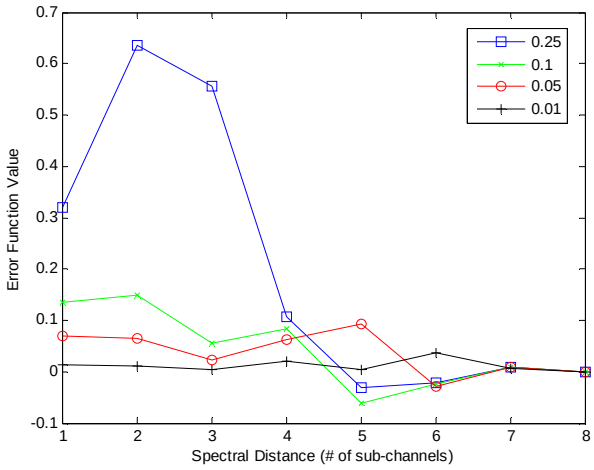

Figure 1. This figure demonstrates the error function value of a pilot sub-channels for all possible placement positions. The model of interference from the PU is that of a wideband one where the PU's bandwidth is equivalent to 20 times of that of the SU's sub-channel bandwidth.

Fig. 1 shows the error function values for possible sub-channel positions of the pilot sub-channel. The different graphs also represent the different interference thresholds in Table 1. This is done for the wideband PU case.

It is noted that in Fig. 1 the optimal pilot position shifts farther away from the PU as the interference threshold decreases. This can be attributed to the stringency of the threshold constraint forcing the pilots to be placed farther away due to the needed reduction of spectral roll-off from the pilot sub-channels.

Another interesting observation which can be noted in Fig. 1 is that for sub-channels 7 and 8, the error function value is almost identical for all 4 interference threshold parameter values and it seems to converge to a point. This

 ISBN: 978-1-61208-131-1

can be attributed to the optimal power loading algorithm and the finite, maximum transmission power which can be loaded per sub-channel. Since the power loading algorithm has reached the point where power assigned to the sub-channel is capped, the whole factor of power loading has effectively been removed from the error function's equation and the power at those points assumes a uniform loading profile (or a water-filling profile for data sub-channels). This means that the error function's value from sub-channels 7 and onwards purely depend on the auto-correlation between pilot symbols and the cross-correlation between pilot symbols and data symbols such that the algorithm becomes irrelevant and the values at any further positions need not be computed so as to save on computational time.

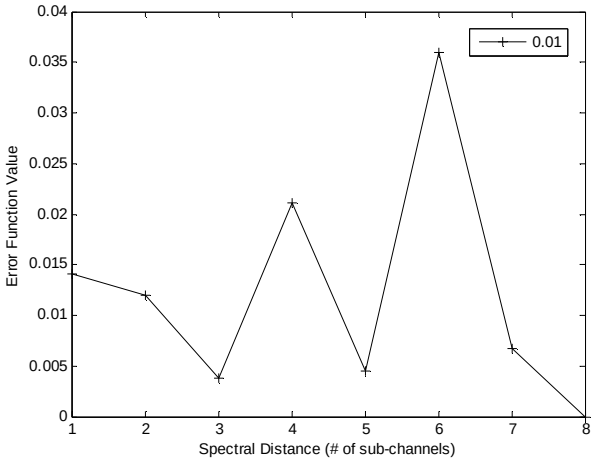

Figure 2. This figure represents the error function value for all possible pilot sub-channel placement positions for an interference threshold of 1 %. The graph is zoomed in for the threshold value from Fig. 1.

Fig. 2 demonstrates the error function value as seen in Fig. 1 for 1% interference threshold while zoomed in on the graph. The graph shows how the optimal pilot position is at sub-channel 6 (5 sub-channels away from the PU where sub-channel 1 is adjacent to the PU). This graph shows an interesting result in that while there is a clear, optimal position, the numeric difference in values of the error function between the best and second best position is relatively small when compared to the rest of the graphs.

This can be attributed to the low interference threshold parameter as defined for the optimal power loading algorithm. This means that the pilot sub-channel has a lower power assigned to it throughout the possible placement positions such that a placing the pilot anywhere in the solution space will provide a relatively small decrease in MSE.

In a practical implementation scenario, this phenomenon can reach a point where it could be debated as to whether a pilot should be added or whether the decrease in MSE is negligible compared to the loss in data rate for when the sub-channel is converted to a pilot-bearing sub-channel.

In Fig. 3 the system is simulated for the case where a narrowband primary user is transmitting. Upon first inspection, once can easily notice that the interference threshold parameter values are much lower, this is due to the decreased bandwidth of the PU which in turn leads to integration over a smaller period to compute the interference introduced to the PU from the SU. The reduced integration period means that for a fixed threshold value, the total sum of the interference will be less than the wideband scenario due to the smaller area of integration. This means that the pilots will tend to be placed farther away the higher the PU's bandwidth is.

Another observation made from Fig. 3 is the convergence to the same error function value occurring from a distance of 6 sub-channels and greater. This can be attributed to the same reason as explained for Fig. 1.

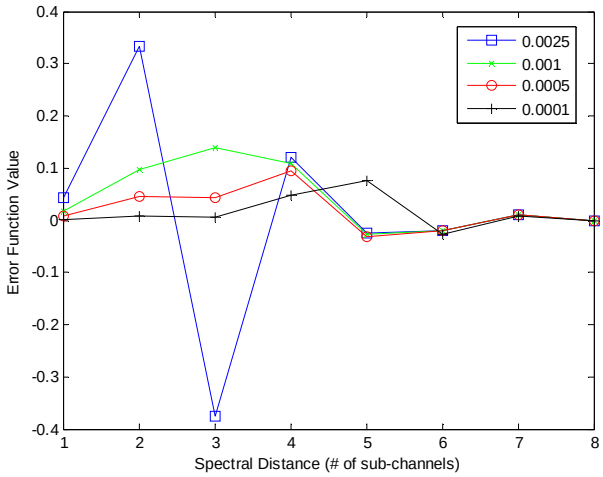

Figure 3. This figure represents the error function value for all possible pilot sub-channel placement positions for the narrowband PU case. The threshold values used are the same as those described in Table 1.

VI. CONCLUSION

The hypothesis investigated in this paper has shown that for the successful implementation of a cognitive radio system, the optimal power loading algorithms and optimal pilot patterns cannot be implemented independently without considering either of them.

It was found that the sub-channels adjacent to the PU cannot simply be converted to pilot sub-channels without any consideration to the optimal power loading algorithms. An error function was therefore derived which allows for the optimal placement of pilots which satisfy interference thresholds while achieving the lowest possible MSE.

The error function was used to compute the optimal pilot placement and was simulated accordingly. It was found that in many cases it is impractical to place the pilot sub-channel adjacent to the PU since the reduction of power required to keep interference to the PU below a threshold mandated a very low SNR on the pilot symbols, leading to a very noisy channel estimate.

It was also found that the interference threshold mandated for the optimal power loading played a big role in

 ISBN: 978-1-61208-131-1

determining the optimal position for the optimal pilot sub-channel position. It was observed that, trivially, as the interference threshold decreased, the pilot sub-channel needed to be placed farther away from the PU such that the threshold condition still is satisfied.

An observation also made was that the error function value for all thresholds converged due to the maximum power which could be allocated per sub-channel due to the power loading algorithm. This meant that the error value did not need to be computed for sub-channels farther than the convergence point.

ACKNOWLEDGMENT

The authors would like to thank Telkom SA, the National Research Foundation (NRF), Technology and Human Resources for Industry Programme (THRIP), the Department of Trade and Industry (DTI), Nokia Siemens Networks and TeleSciences, for supporting this research project.

REFERENCES

[1] J. Mitola III and G. Q. Maguire Jr., "Cognitive radio: making software radios more personal," Personal Communications, IEEE, vol. 6, pp. 13-18, 1999.

[2] I. F. Akyildiz, W. Lee, M. C. Vuran, and S. Mohanty, "NeXt generation/dynamic spectrum access/cognitive radio wireless networks: A survey," Computer Networks, vol. 50, pp. 2127-2159, 9/15, 2006.

[3] V. Valenta, Z. Fedra, R. Marsalek, G. Baudoin and M. Villegas, "Towards cognitive radio networks: Spectrum utilization measurements in suburb environment," in Radio and Wireless Symposium, 2009. RWS '09. IEEE, 2009, pp. 352-355.

[4] G. Bansal, M. J. Hossain and V. K. Bhargava, "Optimal and Suboptimal Power Allocation Schemes for OFDM-based Cognitive Radio Systems," Wireless Communications, IEEE Transactions on, vol. 7, pp. 4710-4718, 2008.

[5] I. Rashad, I. Budiarjo and H. Nikookar, "Efficient pilot pattern for OFDM-based cognitive radio channel estimation - part 1," in Communications and Vehicular Technology in the Benelux, 2007 14th IEEE Symposium on, 2007, pp. 1-5.

[6] T. Weiss, J. Hillenbrand, A. Krohn and F. K. Jondral, "Mutual interference in OFDM-based spectrum pooling systems," in Vehicular Technology Conference, 2004. VTC 2004-Spring. 2004 IEEE 59th, 2004, pp. 1873-1877 Vol.4.

[7] S. Kaiser. (1998, Multi-carrier CDMA mobile radio systems - analysis and optimization of detection, decoding, and channel estimation.

[8] I. Budiarjo, H. Nikookar and L. P. Ligthart, "Performance evaluation of OFDM based cognitive radio system with wiener filter channel estimation using frequency hopping GSM channel model at 900 MHz," in Wireless Technologies, 2007 European Conference on, 2007, pp. 74-77.

 ISBN: 978-1-61208-131-1